steady state would have to be shifted to much more positive values. This goal might be reached if the flatband shift after etching the surface can be avoided. This might be achieved if positive ions which exhibit specific adsorption can be found. Successful attempts in related problems have been mentioned in the literature (8).

Acknowledgments

We would like to thank Dr. O. E. Hüsser for many valuable discussions and Mr. H. Gübeli for the technical assistance. Financial support of the Swiss Federal Office for Education and Science is gratefully acknowledged.

Manuscript submitted Dec. 14, 1987; revised manuscript received May 11, 1988.

Eidgenössische Technische Hochschule Zürich assisted in meeting the publication costs of this article.

REFERENCES

1. J. J. Loferski, *J. Appl. Phys.*, **27**, 777 (1956).
2. M. F. Weber and M. J. Dignam, in "Proceedings of the 5th World Hydrogen Energy Conference," Vol. 3, p. 657, Toronto, Ont., Canada (1984).
3. J. L. Shay and J. H. Wernick, "Ternary Chalcopyrite Semiconductors," Pergamon Press, Ltd., Oxford (1975).
4. D. E. Aspnes, in "Handbook on Semiconductors," M. Balkanski, Editor, North-Holland Pub. Co., Amsterdam (1980).
5. M. Tomkiewicz, W. Siripala, and R. Tenne, *This Journal*, **131**, 736 (1984).
6. R. P. Silberstein, F. H. Pollak, J. K. Lyden, and M. Tomkiewicz, *Phys. Rev. B*, **24**, 7397 (1981).
7. T. Cotting and H. von Känel, *Surf. Sci.*, **162**, 796 (1985).
8. A. Heller, B. Miller, and F. A. Thiel, *Appl. Phys. Lett.*, **38**, 282 (1981).

Perfluorosulfonimide as an Additive in Phosphoric Acid Fuel Cell

M. Razaq, A. Razaq, and E. Yeager*

Case Center for Electrochemical Sciences, Department of Chemistry, Case Western Reserve University, Cleveland, Ohio 44106

Darryl D. DesMarteau and S. Singh

Harvard L. Hunter Chemistry Laboratory, Clemson University, Clemson, South Carolina 29634-1905

ABSTRACT

The addition of 0.5 weight percent (w/o) of the perfluorosulfonimide (PFSI), $CF_3SO_2N(H)SO_2C_4F_9$, as an additive to 85% H_3PO_4 in hydrogen-oxygen fuel cell results in a 70 mV increase in the potential of the oxygen cathode (high surface area, 10% Pt on Vulcan XC-72) at current densities up to 500 mA cm^{-2} at 70°C. This improvement is proposed to be due to the enhanced oxygen reduction kinetics caused by a physically adsorbed layer of the PFSI on the catalyst with the fluorocarbon tail toward the surface. The adsorbed layer creates a "dry cave" environment adjacent to the electrode surface which favors the competitive adsorption of oxygen on the catalyst surface. This adsorbed layer apparently does not interfere with water or proton transfer from or to the interface. Flooding of the gas structure of the porous cathode has not been observed at 0.5 w/o of the PFSI but has been observed at higher concentrations.

Phosphoric acid is the conventional electrolyte for acid hydrogen-oxygen fuel cells because of its relative stability at elevated temperatures, the ease of removal of CO_2 and water, and its surprisingly high conductivity at very high concentrations. However, phosphoric acid has several undesirable characteristics such as its, and/or its anions', strong adsorption on platinum catalyst (1, 2) and lower solubility and diffusivity of oxygen (2, 3). These properties impede the rate of oxygen reduction, and as a result, the polarization of the oxygen cathode is relatively higher. The rate of oxygen reduction in various perfluorinated acids, such as trifluoromethanesulfonic acid, is substantially higher (1, 2, 4-7). This is generally considered to be due to the increased solubility and diffusivity of oxygen and a lower tendency of trifluoromethanesulfonic acid to adsorb on platinum catalyst. However, the use of TFMSA in a practical fuel cell is limited due to its high vapor pressure (8), the ability to wet Teflon-bonded gas-fed electrodes at high concentration (> 6*M*) (4, 8), and lower conductivity (8, 9).

Recently, we reported the possibility of using bis(trifluoromethanesulfonyl)imide as an alternative electrolyte in hydrogen-oxygen fuel cells (3). The oxygen cathode polarization in 84% bis(trifluoromethanesulfonyl)imide at 70°C at 100 mA cm^{-2} was 40 mV lower compared to 85% phosphoric acid. The improved performance of the oxygen cathode in this acid was proposed to be due to the increased oxygen solubility and its relatively weaker adsorption on platinum. The higher oxygen solubility results from the fluorocarbon portion of the electrolyte. The electrolytes with longer fluorocarbon tail(s), however, have lower contact angles with Teflon and they tend to wet Teflon-bonded gas-fed electrodes (10). Therefore, such electrolytes are unsuitable for fuel cell applications using this type of gas-fed electrodes. The present study has been undertaken to establish whether fluorinated electrolytes with longer fluorocarbon tails can be used as additives in phosphoric acid fuel cells. In a mixture with phosphoric acid, perfluorinated electrolytes may form a physically adsorbed layer on the electrode and thus lower phosphoric acid activity and increase oxygen solubility near the catalyst, thereby increasing the rates of the oxygen reduction kinetics. We report here the effects of a perfluorosulfonimide, $CF_3SO_2NHSO_2C_4F_9$, (PFSI), as an additive to 85% phosphoric acid on oxygen electroreduction on smooth as well as high-surface-area platinum gas-fed electrodes. Cyclic voltammetry and rotating disk electrode techniques have been used to study the activity of smooth platinum for oxygen reduction in dilute as well as in 85% phosphoric acid, with and without the presence of the additive. The effects of this additive on the performance of the oxygen cathode in a micro fuel cell at 70°C have also been characterized. The principal factors responsible for the improved performance of the oxygen cathode in the presence of the additive are discussed.

* Electrochemical Society Active Member.

Experimental

Cyclic voltammetry, rotating disk, and current-time transients experiments were performed using either a Pine RDE 3 or PAR 176 Potentiostat and PAR 175 Universal Programmer. The i-E and i-t data were recorded on a YEW Type 3078 X-Y Recorder. For the cyclic voltammetry and rotating disk experiments, a platinum rotating disk electrode (AFDT 22 PTPT, Pine Instruments Company) with an area of 0.126 cm^2 was used. The electrode surface was polished with alumina (0.05 μm) to a mirror finish and then thoroughly washed with distilled water. Prior to recording the cyclic voltammograms, the electrode potential was cycled between 1.4 and 0.02V *vs.* RHE until a steady-state behavior was obtained. Before recording the cyclic voltammetric curves for O_2 reduction on a smooth stationary Pt electrode, the electrode was cleaned by cycling the potential between 1.4 and 0.02V three times and between 1.0 and 0.4V one time at 100 mV s^{-1}. The voltammetry curves for O_2 reduction were then recorded by sweeping the potential from 1.0V at 10 mV s^{-1} in the negative direction. Before recording the polarization curves for oxygen reduction on the rotating disk electrode, the electrode surface was pretreated by stepping the potential between 1.4 and 0.4V (three times). The potential was then stepped to 1.0V and the polarization curve recorded by sweeping the potential at 10 mV s^{-1} in the cathodic direction. This procedure was followed for each rotation rate.

The solubilities and the diffusion coefficients of oxygen were determined using a platinum microdisk electrode (25 μm diam, 99.95% pure platinum, Johnson-Mathey) sealed in glass as the working electrode. The microdisk electrode was polished down to 1 μm with diamond paste of different grade and then polished to mirror finish with 0.05 μm alumina. The electrode was then cleaned with a 1:1 mixture of concentrated nitric and sulfuric acid, followed by thorough rinsing with distilled water. Prior to recording the i-t transients, the electrode was pretreated by stepping the potential between 1.4 and 0.4V (three times), and the i-t transients were then recorded by stepping the potential from 1.0V, where the oxygen reduction is negligible, to 0.4V, where oxygen reduction is assumed to be diffusion controlled. This procedure yielded reproducible data.

The counterelectrode was a platinum flag. An *in situ* dynamic hydrogen electrode was used as a reference electrode. The experiments were performed in a conventional type of two-compartment, three-electrode glass cell. The reference electrode was in a compartment separated from the working electrode by a Luggin capillary. All measurements were made at room temperature unless otherwise stated.

The micro fuel cell used for obtaining the galvanostatic i-E curves for oxygen reduction was made of Kel-F and has been described elsewhere (3). The cathode and the anode used in the fuel cell were high-surface-area Prototech standard gas diffusion electrodes [10% Pt loading on carbon (Vulcan XC-72)] with an area of ~250 m^2/g. The fuel cell was operated under temperature control in an air thermostat (temperature-controlled drying oven). The i-E curves were recorded point-by-point using a Stonehart Associate BC 1200 potentiostat and a Hi-Teck PPR1 waveform generator.

The 85% phosphoric acid was of Analar grade and was further purified using the procedure described elsewhere (11). The PFSI was prepared by literature method (12). The

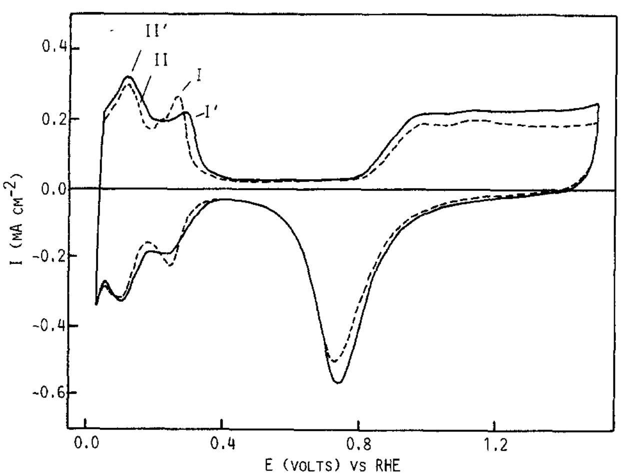

Fig. 1. Voltammograms of Pt in 0.1M PFSI (———) and 0.1M H_3PO_4 (------) solutions saturated with N_2. Sweep rate = 100 mV s^{-1}; *T* = 20°C.

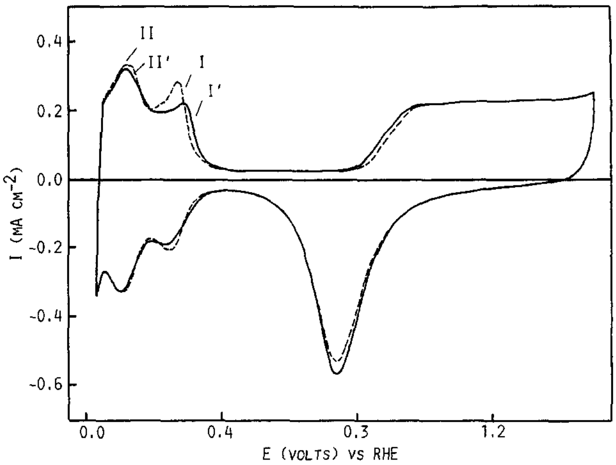

Fig. 2. Voltammograms of Pt in 0.1M PFSI (———) and 0.1M PFSI containing 20 mM H_3PO_4 (------) solutions saturated with N_2; sweep rate = 100 mV s^{-1}; T = 20°C.

distilled water used in this work was prepared by reverse osmosis of tap water followed by distillation with a counter flow of nitrogen to purge volatiles such as carbon dioxide and organics.

Results and Discussion

The voltammetry curves for platinum in dilute as well as in concentrated phosphoric acid with and without the presence of PFSI were recorded to see the effects of anion adsorption on the activity of platinum. Figure 1 shows the voltammetry curves of platinum in 0.1*M* solutions of phosphoric acid and of PFSI all saturated with purified nitrogen. The voltammetry curves are similar but not identical. The voltammetry curves differ significantly in the hydrogen adsorption-desorption and the oxide regions. The onset of oxide formation in the anodic sweep occurs at more negative potential in the case of PFSI relative to phosphoric acid. Furthermore, the currents in the oxide formation region and its reduction are higher for the PFSI. This is an indication of weaker adsorption on Pt by the PFSI relative to phosphoric acid. There is a significant anodic shift in the hydrogen adsorption-desorption region (peak I) for the PFSI. Also, as observed in the case of weakly adsorbed acids (13), *e.g.*, $HClO_4$, the peak current for the strongly adsorbed form of hydrogen on Pt is lower for the PFSI than for the phosphoric acid. The coupling of the hydrogen adsorption and the desorption of the anions

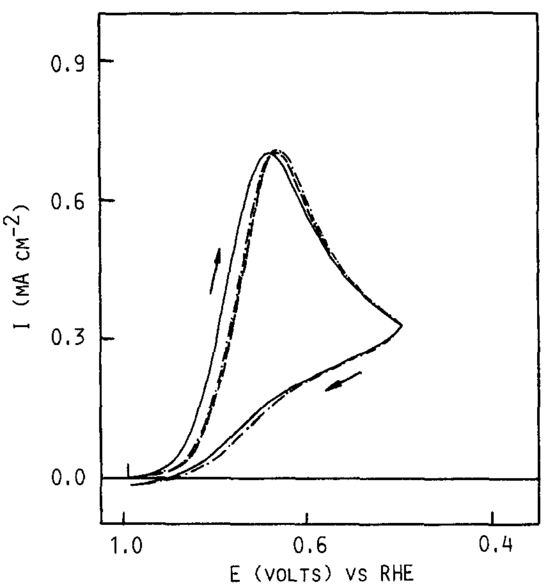

Fig. 3. Voltammograms of Pt for O_2 reduction in 0.1M solutions of PFSI (———), H_3PO_4 (------), and 0.1M PFSI containing 20 mM H_3PO_4 (- · - · - ·); solutions saturated with O_2 at 1 atm.; sweep rate = 10 mV s^{-1}; *T* = 20°C.

leads to a very sharp peak for hydrogen adsorption with high peak current, although the charge under the peak remains the same. Upon addition of 25 m*M* phosphoric acid in 0.1*M* PFSI, the anodic shift of peak I in the hydrogen adsorption region and the cathodic shift in the oxide formation region seen for the PFSI have disappeared and the voltammogram becomes similar to that obtained in 0.1*M* phosphoric acid (Fig. 2). This suggests that the phosphoric acid has at least partially displaced the PFSI from the electrode surface.

Figure 3 shows the voltammetry curves for oxygen reduction in 0.1*M* solutions of phosphoric acid and PFSI all saturated with oxygen. A single irreversible wave corresponding to oxygen reduction is observed prior to the hydrogen adsorption peaks. The peak current density for both solutions is the same, suggesting that the oxygen solubility in dilute phosphoric acid and PFSI is the same. However, the half-wave potential, $E_{1/2}$ (the potential corresponding to 85% of the peak current) for the PFSI is 30 mV more positive compared to the $E_{1/2}$ observed for the phosphoric acid. This suggests that due to the relatively weaker adsorption of the PFSI on Pt, more active sites are available to interact with oxygen. Upon addition of 20 m*M* phosphoric acid in 0.1*M* PFSI, the $E_{1/2}$ value becomes the same as in 0.1*M* phosphoric acid. This indicates that to some extent, even such a low concentration of the phosphoric acid has partially blocked the active Pt sites. The *p*H also influences the oxygen reduction potentials (14). The *p*H of the 0.1*M* PFSI on the addition of 25 m*M* phosphoric acid changed from 1.20 to 1.25. Therefore, the shift in the half-wave potential for oxygen reduction in 0.1*M* PFSI in the presence of 25 m*M* phosphoric acid is predominantly due to the blocking of the active Pt sites by the relatively strongly adsorbed phosphoric acid.

Figure 4 shows the voltammetry curves for Pt in 85% phosphoric acid and 85% phosphoric acid containing 4 w/o (0.156*M*) of the PFSI solutions saturated with nitrogen. The mixture is an emulsion with a milky appearance. The voltammetry curves are similar with the exception that in the presence of PFSI, there is a slight anodic shift in the hydrogen adsorption region and the onset for the oxide formation occurs at slightly more negative potentials. Furthermore, the currents for the oxide formation and its reduction are slightly higher.

Figure 5 shows the polarization curves for oxygen reduction on a Pt rotating disk electrode in 85% phosphoric acid and 85% phosphoric acid containing 4 w/o PFSI solutions saturated with oxygen. There is a 90 mV positive shift in the half-wave potential at a given rotation rate of 400 rpm for oxygen reduction in the mixture as compared to the half-wave potential observed in 85% phosphoric acid alone. The limiting current densities (calculated by plotting 1/I *vs.* $1/\omega^{1/2}$) in the mixture are also higher by a factor of 1.64 compared to 85% phosphoric acid alone.

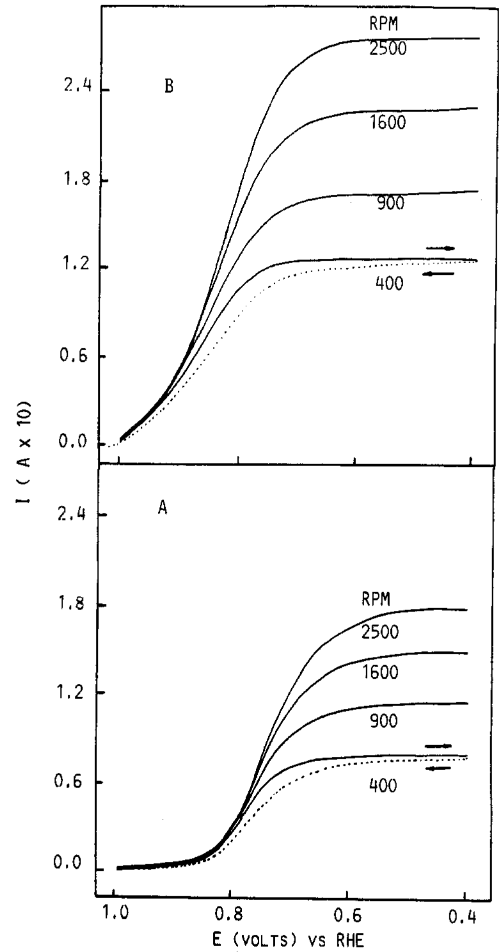

Fig. 5. (a) Polarization curves for O_2 reduction on a Pt rotating disk electrode (area = 0.126 cm^2) in 85% H_3PO_4; solution saturated with O_2 at 1 atm; sweep rate = 10 mV s^{-1}; T = 20°C. (b) Solution 85% H_3PO_4 + 4% PFSI. Other conditions same as for Fig. 5a.

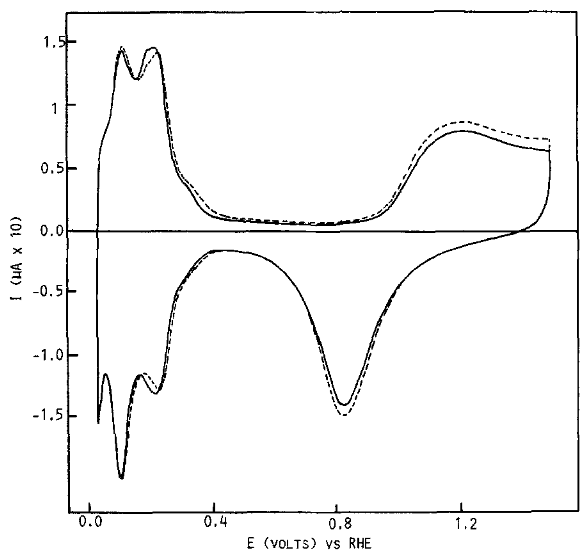

Fig. 4. Voltammograms of Pt in 85% H_3PO_4 (———) and 85% H_3PO_4 containing 4% PFSI (- - - - - -) solutions saturated with N_2; sweep rate = 100 mV s^{-1}; electrode area = 0.126 cm^2; T = 20°C.

The platinum activity for oxygen reduction in dilute and concentrated mixtures is strikingly different. This may be explained by the following discussion.

The dilute solution mixture (0.1*M* PFSI containing 0.02*M* H_3PO_3) is homogenous. The phosphoric acid in the mixture has a relatively higher tendency to adsorb on Pt than the PFSI. As a result, the oxygen reduction kinetics in the mixture are slower compared to the 0.1*M* PFSI alone. Ross and Andricacos (7) have reported similar effects of phosphoric acid on oxygen reduction kinetics on Pt in trifluoromethanesulfonic acid. They attributed the slower oxygen reduction in the presence of phosphoric acid as due to the site blocking by the phosphoric acid and its anions and a rise in the activation energy barrier. The concentrated mixture of acids (85% H_3PO_4 containing 4% PFSI) is an emulsion. At higher concentrations, phosphoric acid has a strong hydrogen-bonded network structure, and it squeezes out the PFSI which forms a physically adsorbed layer on a solid surface, *e.g.*, the electrode with fluorocarbon tails toward the metal and the polar end toward the bulk phosphoric acid (due to the dipole-dipole interactions). The PFSI layer at the electrode-electrolyte interface reduces the activity of phosphoric acid at the electrode surface. This layer is like a "dry cave" in which oxygen has higher concentration than in the bulk phosphoric acid, and in which the phosphoric acid and water are in lower concentration. This "dry cave" environment adjacent to the electrode surface increases the rate for the oxygen reduction. The PFSI layer may be only a single molecule thick and does not seemingly interfere with oxygen and water/proton transport across the interface. This layer in some ways resembles Langmuir-Blodgett film with the fluorocarbon end toward the metal.

The PFSI is a stronger acid (pKa = 0.91) than phosphoric acid (pKa = 2.15). However, the solubility of the PFSI in 85% H_3PO_4 is less than 0.5%, and the amount of the PFSI greater than 0.5% forms an emulsion with 85% H_3PO_4. The addition of 4% of the PFSI would suppress the ionization of only a small fraction of the phosphoric acid. Hence the *p*H would not change significantly. The hydrogen evolution potential was checked against a $Hg/Hg_2(H_2PO_4)_2$, 85% H_3PO_4, reference electrode. The junction potential between 85% H_3PO_4 and 85% H_3PO_4 containing 4% PFSI should be negligible. No change in the hydrogen evolution potential in the mixture was observed. This indicates that no significant change in the *p*H of 85% H_3PO_4 was produced by the addition of 4% of the PFSI. Therefore, the large shift in the half-wave potential for oxygen reduction observed in 85% H_3PO_4 containing 4% of the PFSI (Fig. 5) is not due to the change in the *p*H of the mixture.

It is interesting to note that the current in the diffusion-limited region undergoes considerable fluctuation in the mixture, but not in 85% phosphoric acid alone, when oxygen is bubbled near the electrode (Fig. 6). Apparently, with the presence of the surfactant-like PFSI, the oxygen bubbles, as they drag across the electrode surface, produce local variation in the hydrodynamic boundary layer and the Nernst layer, thus causing a noise signal. In the presence of the PFSI, the oxygen bubbles approach close to the surface and hence have the large effect on the boundary layer.

The production of H_2O_2 in the mixture, as well as in 85% phosphoric acid, was also monitored at the ring electrode by holding the ring potential at 1.1V while sweeping the disk potential from 1.0 to 0.4V. The ratios of the disk current to ring current were similar, suggesting that the additive had no significant effect on the overall mechanism for oxygen reduction.

The increase in the limiting current density in the rotating disk experiment with 4 w/o of the additive is a surprisingly large effect considering the small concentration of the additive. The limiting current depends on the solubility, diffusion coefficient as well as on the thickness of the Nernst boundary layer. All of these can be influenced by the additive.

The solubility and diffusivity of oxygen in 85% phosphoric acid and 84% PFSI were determined using a microelectrode technique (15). The intercept and the slope of i *vs.* $t^{-1/2}$ plot are related to the solubility and diffusion coefficient by the equations given by Winlove *et al.* (15).

$$D_{O_2} = a^2A^2/\pi B^2 \quad [1]$$

$$C_{O_2} = B^2/n\mathbf{F}Aa^3 \quad [2]$$

where A is the intercept, B is the slope, a is the radius of the microdisk, n is the number of electrons transferred, and $\mathbf{F}$ is the Faraday constant. A typical i *vs.* $t^{-1/2}$ plot for oxygen reduction in 84% PFSI is shown in Fig. 7. The solubility and the diffusion coefficient of oxygen calculated by using Eq. [1] and [2] are $4.73 \times 10^{-3} M\,l^{-1}$ and 5.97×10^{-6} cm^2 s^{-1}, respectively. The solubility and the diffusion coefficient of oxygen in PFSI are much higher than in phosphoric acid (see Table I) by an order of magnitude in the instance of the solubility and fivefold for the diffusion coefficient. Since $I_L \propto CD^{2/3}/\nu^{1/6}$, the limiting current is not sensitive to the kinematic viscosity. The difference in the $CD^{2/3}$ product for 85% H_3PO_4 and 84% PFSI would explain the 1.64-fold increase in the current density observed with the rotating disk experiment in 85% H_3PO_4 containing 4 w/o of the additive (Fig. 5).

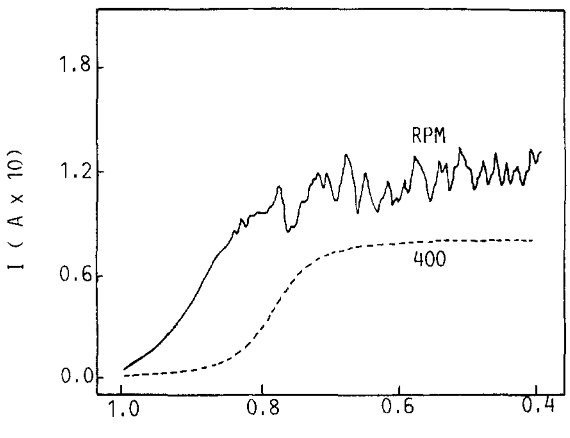

Fig. 6. Polarization curves for oxygen reduction on a Pt rotating disk electrode in 85% H_3PO_4 (———) and 85% H_3PO_4 containing 4% PFSI (- - - - -) while bubbling O_2 near the electrode. Other conditions same as for Fig. 5a.

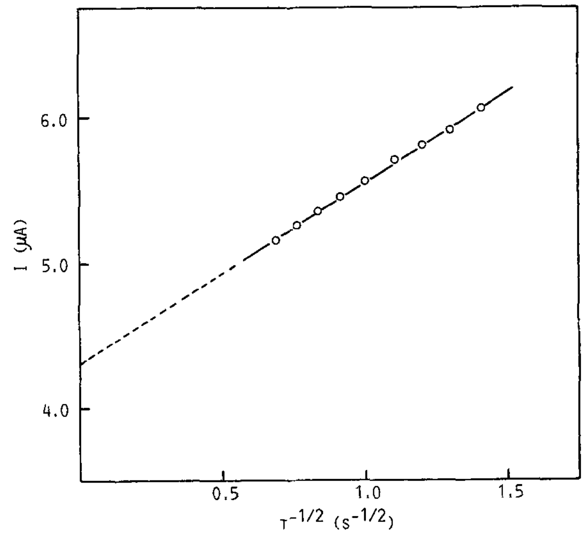

Fig. 7. The plot of i *vs.* $t^{-1/2}$ for oxygen reduction in 84% PFSI on Pt microelectrode (diam = 25 μm) for a potential step from 1.0 to 0.4V; *T* = 20°C.

The performance of the oxygen cathode (Prototech standard gas-diffusion electrode, 10% Pt on Vulcan XC-72) was checked in the microfuel cell in 85% H_3PO_4 containing different w/o ratios of PFSI at 70°C using pure oxygen at 1 atm. The galvanostatic i-E curves were corrected for the iR drop using the current interrupter method (16). The i-E curves were recorded point-by-point with increasing current. The performance of the cathode was highly dependent on the total content of PFSI in the 85% H_3PO_4. Figure 8 shows the polarization curve for oxygen reduction in the 85% H_3PO_4 and 85% H_3PO_4 containing 4% PFSI. The polarization of the cathode in the lower current density region is lower than in 85% H_3PO_4 alone. However, the polarization of the cathode increases rapidly beyond 0.5 mA cm^{-2}. This is a typical response of a gas-fed electrode being run under flooded conditions. The 4% PFSI apparently results in the flooding of the gas-fed electrode. In a mixture containing 2 w/o PFSI, the performance of the cathode initially is similar to that in 85% H_3PO_4 alone. However, the cathode potential decreases with time, and in 3h, the potential decreases from 800 mV to 510 mV (*vs.* RHE) at 20 mA cm^{-2} (Fig. 9). This increase in the cathode polarization is due to the slow flooding of the gas fed cathode with time.

In 85% H_3PO_4 containing 0.5% of the PFSI, the polarization of the cathode is much lower than in 85% phosphoric acid alone; at 100 mA cm^{-2}, the cathode potential is 70 mV more positive as compared to 85% phosphoric acid alone (Fig. 10). The polarization curve is time independent (in the 48h time scale of the experiment) which suggests that in this mixed electrolyte, the amount of PFSI is lower than the critical value which could cause flooding of the gas-fed

Table I. The solubility and the diffusion coefficient of oxygen in phosphoric acid and PFSI

Electrolyte	Solubility $M\,l^{-1}$	Diffusion coefficient cm^2 s^{-1}
85% H_3PO_4	3.3×10^{-4}	1.21×10^{-6}
84% PFSI	4.7×10^{-3}	6.53×10^{-6}

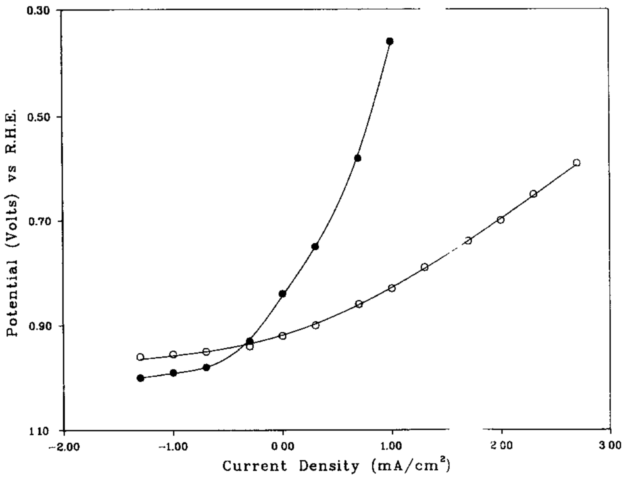

Fig. 8. Polarization curves for O_2 reduction on high-surface-area Prototech standard gas-fed electrode (10% Pt on Vulcan XC-72) in 85% H_3PO_4 (○) and 85% H_3PO_4 + 4% PFSI (●) at 70°C.

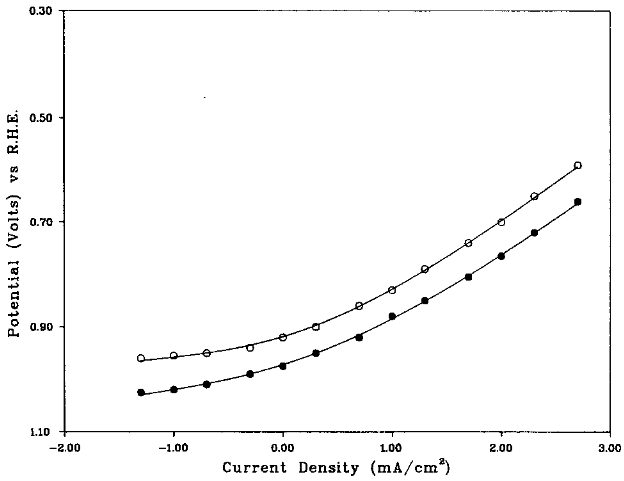

Fig. 10. Polarization curves for O_2 reduction on high-surface-area Prototech standard gas-fed electrode in 85% H_3PO_4 (○) and 85% H_3PO_4 containing 0.5% PFSI (●) at 70°C.

electrodes. Below this concentration, *e.g.*, 0.125 w/o of the PFSI, the cathode potential is still higher than phosphoric acid, but the effect of the additive is less prominent (Fig. 11). The stability of the PFSI in 85% H_3PO_4 at higher temperatures (>150°C) was checked by heating the mixture in a beaker. After 5h, starting with 4% of the PFSI in 85% H_3PO_4, a substantial amount of the PFSI was lost due to evaporation. No attempts were made to run the fuel cell at temperatures higher than 70°C.

Conclusion

The voltammetry studies of Pt in 0.1*M* PFSI solutions containing 20 m*M* phosphoric acid show adverse effects of the phosphoric acid on the oxygen reduction kinetics. On the contrary, 85% phosphoric acid containing even just 0.125 w/o of PFSI results in a substantially higher Pt activity for oxygen reduction. This may be interpreted on the basis that the PFSI forms a physically adsorbed layer on the electrode surface. Considering the two distinct parts of the PFSI (fluorocarbon tail and the sulfonimide group), the probable orientation of PFSI on the electrode surface is with the fluorocarbon end toward the metal while the polar group is toward the bulk phosphoric acid. The detailed structure and the thickness of the PFSI layer cannot be elucidated at this stage. The use of some *in situ* methods such as SERS and EMIRS/SNIFTIRS may be necessary to address these questions. The physically adsorbed layer of the PFSI on the electrode creates a "dry cave" environment adjacent to the electrode surface in which oxygen has higher concentration compared to bulk phosphoric acid and in which water and phosphoric acid are in lower concentration. The hydrophobic part of the PFSI being toward the surface may change the dielectric constant near the electrode surface in such a way as to favor the competitive adsorption of O_2 on platinum. This is believed to be the major factor responsible for the enhanced kinetics for oxygen reduction as observed on both the smooth Pt disk (Fig. 5) and high-surface-area Pt gas-fed electrodes (Fig. 10).

A 70 mV decrease in the polarization of the oxygen cathode in the fuel cell in the presence of 0.5 w/o of the PFSI is very encouraging and could be very useful in fuel cell applications. The optimum w/o ratio of PFSI may, however, depend on the electrode/solution volume ratio and the nature of the gas-fed electrodes; the micropore size (gas wicks) in the gas-fed electrodes depends on the method of fabrication. The PFSI content should be sufficient to form a monolayer on the catalyst, but should not exceed the concentration where it could fill the gas wicks.

With the relatively lower surface tension of 85% H_3PO_4 in the presence of the PFSI, the gas-fed electrode would have better wetting properties which could result in a better performance of the cathode. However, a positive shift in the $E_{1/2}$ for oxygen reduction on a smooth Pt rotating disk electrode suggests that the superior performance of the gas-fed cathode in the presence of the PFSI is not only due to the better wetting of the catalyst, but also is due to the modified electrode/electrolyte interface.

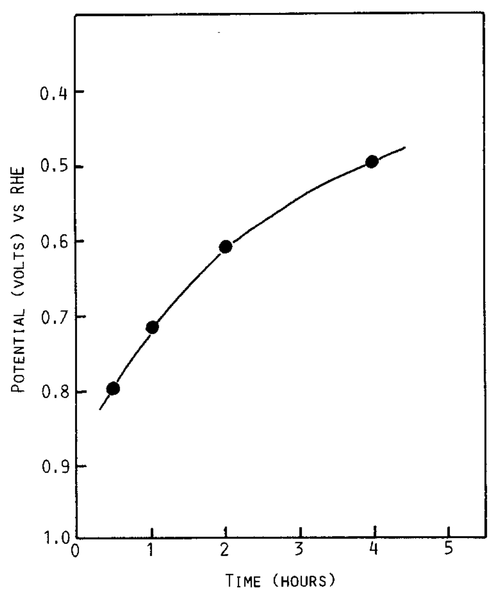

Fig. 9. Time dependence of the cathode potential for O_2 reduction on Prototech standard gas-fed electrode in 85% H_3PO_4 containing 2% PFSI at 20 mA cm^{-2}; $T = 70°C$.

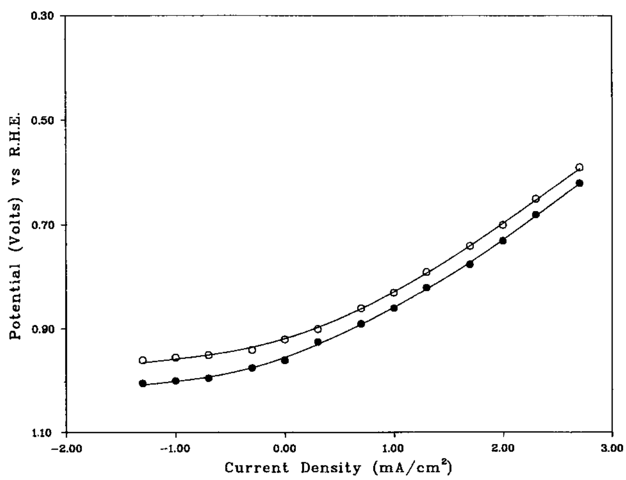

Fig. 11. Polarization curves for O_2 reduction on high-surface-area Prototech standard gas-fed electrode in 85% H_3PO_4 (○) and 85% H_3PO_4 containing 0.125% PFSI (●) at 70°C.

Some researchers (17, 18) have proposed the replacement of the liquid-concentrated phosphoric acid in gas-fed porous O_2 consuming cathodes, with ionic conducting polymers such as Nafion with the advantage of speeding up the kinetics of the oxygen reduction reaction by a mechanism similar to that proposed for the role of the PFSI addition. The use of additives such as PFSI has several advantages over the polymer including: (*i*) greater ease of access to the porous gas-fed electrode; (*ii*) self-healing in that the surface film, if disturbed, is automatically healed by the adsorption of the additive from the bulk solution; and (*iii*) it has essentially the same conductivity as concentrated phosphoric acid without the additive, in contrast to the polymer which, with its lower conductivity, gives rise to additional ohmic losses within the electrode.

The vapor pressure of the PFSI itself is too high for operating under the practical fuel cell conditions (150°-200°C). A condenser system could be used to recover the vaporized PFSI, but this would add substantial complications to the system. An alternative approach is to identify less volatile additives suitable for operating at higher temperatures. Work is in progress in our laboratory to substitute the PFSI by low volatile multifunctional perfluorosulfonimide, perfluorinated phosphonic, or phosphinic acids which could be used as additives in phosphoric acid at higher temperatures.

Acknowledgment

This research has been supported by the Gas Research Institute, Chicago, Illinois.

Manuscript submitted Aug. 17, 1987; revised manuscript received May 10, 1988.

Case Western Reserve University assisted in meeting the publication costs of this article.

REFERENCES

1. A. J. Appleby and B. S. Baker, *This Journal*, **125,** 404 (1978).
2. P. Zelenay, B. R. Scharifker, J. O'M. Bockris, and D. Gervasio, *ibid.*, **133,** 2262 (1986).
3. M. Razaq, A. Razaq, E. Yeager, D. D. DesMarteau, and S. Singh, *J. Appl. Electrochem.*, In press.
4. M. A. Enyattullah, Ph.D. Thesis, Case Western Reserve University (1986).
5. A. A. Adams, R. T. Foley, and H. J. Barger, Jr., *This Journal*, **124,** 1230 (1977).
6. S. Srinivasan and F. J. Salzano, Paper presented at the ERDA-EPRI Fuel Cell Seminar, Palo Alto, CA, June 29-July 1, 1976.
7. P. N. Ross and P. C. Andricacos, *J. Electroanal. Chem.*, **154,** 205 (1983).
8. M. George and S. Januszkiewicz, Final Report, Energy Research Corporation, Danbury, CT 06810, ERC-0123-F (June 1977).
9. R. Corkum and J. Milu, *Can. J. Chem.*, **56,** 1832 (1978).
10. M. Razaq, A. Razaq, and E. Yeager, To be published.
11. J. C. Huang, R. K. Sen, and E. Yeager, *This Journal*, **126,** 786 (1979).
12. D. D. DesMarteau and S. Singh, To be published.
13. J. C. Huang, W. E. O'Grady, and E. Yeager, *This Journal*, **124**, 1732 (1977).
14. M. R. Tarasevich, A. Sadkowski, and E. Yeager, in "Treatise of Electrochemistry," Vol. 7, B. Conway, J. O'M. Bockris, E. Yeager, S. U. Khan, and R. White, Editors, Plenum Press, New York (1983).
15. C. P. Winlove, K. H. Parker, and R. K. C. Oxenham, *J. Electroanal. Chem.*, **170,** 293 (1984).
16. Southampton Electrochemistry Group in, "Instrumental Methods in Electrochemistry," p. 379, Ellis Harwood, Ltd., Chichester (1985).
17. E. Yeager, D. Chu, and D. Gervasio, EPRI Workshop on Fuel Cell Technology, Feb. 17, 1987, Clearwater, FL (1987).
18. I. D. Raistrick, Abstract 450, p. 660, The Electrochemical Society Extended Abstracts, Vol. 86-1, Boston, MA, May 4-9, 1986.

The Effect of Suspended Solids on Mass Transfer to a Rotating Disk

P. K. Andersen,*[,1] R. H. Muller,* and C. W. Tobias*

Department of Chemical Engineering and Materials and Chemical Sciences Division, Lawrence Berkeley Laboratory, University of California, Berkeley, California 94720

ABSTRACT

The enhancement of limiting currents by inert suspended solids was studied using a rotating-disk electrode (RDE). The suspensions contained glass or polymer particles in various sizes (1-100 μm) and concentrations (up to 40 v/o solids). Solid particles the same size as, or smaller than, the thickness of the mass-transfer boundary layer create small-scale "microconvective" vortices. Particles much larger than the boundary-layer thickness appear to enhance transport by a different mechanism, possibly involving the formation of particle-free wall layers. Disk-torque measurements show that substantial increases in the limiting current require significantly less stirring power using the suspensions than by increasing the rotation rate without solids.

The addition of inert solid particles to a flowing liquid can increase wall mass-transfer rates several-fold, depending on such factors as the particle size, the shear rate, and the volume fraction of solids (1-5). In the absence of hydrodynamic effects, the inert particles might be expected to reduce transport rates by acting as obstacles to the diffusion of solutes in the electrolyte. Thus, for diffusion in stationary solid-liquid suspensions, Prager (6) showed that the effective diffusivity $D^\bullet$ may be related to the true diffusivity D by

$$\kappa \equiv \frac{D^\bullet}{D} = 1 - \frac{3}{2}\phi + \frac{1}{2}\phi^2 \qquad [1]$$

where ϕ is the volume fraction of solids. As expected, $D^\bullet \to 0$ as $\phi \to 1$.

Equation [1] cannot be expected to predict the effective diffusivity in a flowing suspension. When a suspension is sheared, the solid particles create local "microconvective" flows, superimposed on the bulk flow field, which increase both the dispersion of solutes and the dissipation of energy. These secondary flows are usually thought to result from the rotation of the solid particles (2, 4, 5). It is well known that an isolated solid particle immersed in a viscous fluid will tend to rotate with an angular velocity one-half the bulk shear rate $\dot{\gamma}$. It should be noted, however, that as ϕ increases, each particle comes into more frequent contact with its neighbors, and is consequently unable to rotate freely. Even at ϕ = 5%, nearly a third of the particles may exist as "collision doublets" at any one time (7). Stud-

* Electrochemical Society Active Member.
[1] Present address: School of Chemical Engineering, Purdue University, West Lafayette, Indiana 47907.